Melt-derived copper-doped ferrimagnetic glass-ceramic for tumor treatment

Melt-derived copper-doped ferrimagnetic glass-ceramic for tumor treatment

Marta Miola[1]*, Matteo Bruno[1], Roberto Gerbaldo[1], Francesco Laviano[1], Enrica Vernè[1]

[1] Politecnico di Torino, Applied Science and Technology Department, Corso Duca degli Abruzzi 24, 10129 Torino, Italy

* **Corresponding author:**

Dr. Marta Miola

Politecnico di Torino

Department of Applied Science and Technology (DISAT)

Corso Duca degli Abruzzi 24, 10129 Torino, ITALY

Tel.: +39-0110904717

Fax: +39-0110904624

e-mail: marta.miola@polito.it

Keywords

Ferrimagnetic glass-ceramic; copper; bone tumor; infection prevention

Abstract

Copper-containing ferrimagnetic glass-ceramic was synthesized by means melt and quenching process both in powder and bulk form. The obtained samples were characterized by means morphological, compositional and structural analyses. The magnetic properties and the ability to release heat were also investigated together with the antimicrobial properties towards *S. aureus* strain. The obtained results showed that copper introduction and the annealing process influenced the nucleation of crystalline phases; in particular the samples produced in powder form evidenced a low amount of magnetite and thus a reduced hysteresis area and ability to produce heat when exposed to an alternating magnetic field. While Cu-containing samples in the bulk form maintained the magnetic and calorimetric properties of pristine glass-ceramic. Preliminary evaluation of antibacterial properties demonstrated Cu-doped samples were not able to reduce the bacterial proliferation and thus the need to optimize the copper introduction process.

1. Introduction

The incidence of malignant bone tumors is relatively low, however the mortality connected to this pathology is extremely high. Actually, they are mainly treated with surgery and traditional therapies, such as chemotherapy and radiotherapy [1,2]. The surgery procedure is very invasive and causes high morbidity; it consists in a wide local excision or amputation and in a resulting reconstruction of the excised tissue with an implant (e.g. metallic prosthesis, acrylic bone cement, allograft or autograft) that often implies risks of infection in already immunocompromised patients [3]. Even though the treatment of benign bone tumours is less aggressive, also in this case the use of an implant is the common adopted solution.

To overcome these drawbacks and limit the side effects connected to chemotherapy and radiotherapy, innovative treatments have been exploited, such as immunotherapy, targeted therapy and gene therapy [4,5]. Among these new solutions, hyperthermia, and in particular magnetic hyperthermia, is deeply investigated [6-8]. Hyperthermia includes several techniques that exploit the use of heat to destroy tumors (temperatures > 41-42 °C). The mechanism of hyperthermic treatment consists in the increase of tissues

temperature between 42-46 °C (e.g. by means of microwave or radiofrequency devices); tumoral cells and tissues are more sensitive to heat than normal ones, because tumoral tissues are characterized by a poor vasculature and unresponsive microvasculature that hinder the heat dissipation by blood flow and act as heat-reservoir. Moreover, hyperthermia can decrease the intratumor pH and this decrease would promote the heat effect on tumoral cells [9,10] and act at cellular level causing several macromolecular changes [11]. It has been also demonstrated that hyperthermia enhance the effect of both chemotherapy and radiotherapy, by improving the cells sensitization to ionizing radiation and antineoplastic agents [10-12].

Magnetic hyperthermia, a treatment based on the developing of heat by a magnetic material subjected to an alternating magnetic field, has been also investigated by exploiting different magnetic materials, such as iron oxides, ferrites, metal alloys [13,14]. Among the magnetic materials, magnetic glass-ceramics have drawn the attention of the researchers [15-22]. In particular, bioactive magnetic ceramics have been investigated in the treatment of tumor-related bone loss, due to material ability to destroy tumoral cells and, at the same time, to promote the precipitation of hydroxyapatite and, in turn, to stimulate the osteointegration of the implant [ref]. Different bioactive magnetic and bioactive glass-ceramics compositions synthesized by melt and quenching process or via sol-gel have been investigated, in different forms and structures (bulk, powders, mesoporous), for different tumoral tissues especially bone tissue [15-26]. The ability of magnetic and bioactive glass-ceramics to be functionalized or loaded with antineoplastic drugs have been also exploited [27], as well as the possibility to be used as filler in bone cement [28-30]. Moreover, glasses and glass-ceramics composition can be easily modified by introducing ions with therapeutic effect [31-33], both during the materials synthesis (e.g. as precursors during the melt and quenching or sol-gel process) [34-36] or after the materials synthesis (e.g. by means of ion exchange technique) [37-39].

A common problem connected to the surgery of bone tumors is the development of infections [40,41], especially in patients already immunocompromised due to radio and chemotherapies. For this reason, the authors modified a bioactive and ferrimagnetic glass-ceramic by introducing elements with antimicrobial effect. In a previous work, Miola et al. evaluated the effect of silver introduction in a bioactive and ferrimagnetic glass-ceramic in terms of morphology, structure, magnetic and antibacterial properties [42].

Due to the recent discovery and growing evidence of bacterial resistance to silver, connected to the widespread use of silver-containing devices [43], in this research work the authors verified the possibility to incorporate copper in the composition of a bioactive and ferrimagnetic glass-ceramic. Copper was inserted as reactant during the melt and quenching process and the authors verified the effect of its introduction in the glass-ceramic morphology, microstructure, the ability to generate heat, the magnetic and antimicrobial properties.

2. Materials and method

2.1 Glass-ceramics synthesis

A ferrimagnetic glass-ceramic (SC45) with the following composition: 24.7% SiO_2-13.5% CaO-13.5% Na_2O-3.3% P_2O_5-31% Fe_2O_3-14% FeO (wt%) was produced by melt and quenching technique as previously reported [26,42]. Briefly, the reactants were mechanically mixed and melted in a Pt crucible at 1550 °C (Nabertherm-Carbolite 1800, Italy), then melt was poured in a brass mold. A fraction of the melt was subsequently milled and sieved to obtain powders with particles size below 20 μm; another fraction was quenched in a brass mould to obtain bars, which were annealed at 600 °C for 12 h and cut in slices of 10x10x1.5 mm^3; subsequently, the sheets were polished with SiC abrasive papers up to 1200 grit.

In order to introduce copper in the SC45 composition, CuO was introduced as reactant during the melt and quenching process. The Cu-doped SC45 (SC45_%Cu) contains 5% wt% of CuO in place of CaO and was synthesized using the same procedure described for SC45. Also in this case both powders (< 20 μm) and slices of 10x10x1.5 mm^3 were produced.

In both cases, crystal phases nucleated and grow during cooling, originating unconventional glass-ceramic materials. All reagents for glass ceramics preparation were purchased by Sigma Aldrich.

2.2 Glass-ceramics characterization

The morphology and composition of SC45 and SC45_5Cu were analyzed by means of field emission electron microscopy (FESEM – SUPRATM 40, Zeiss) equipped with energy dispersion spectrometry (EDAX PV 9900). Samples were chromium-coated prior to the analysis. The FESEM-EDS analysis was performed also on samples subjected to a chemical etching using fluoridric (HF) and nitric acids (HNO_3) in 1:1 molar ratio and a water/acid solution (5% v/v), in order to enhance the visualization of crystalline phases. The samples were put in 20 ml of water/acid solution and left for 1 minute. Subsequently, they were washed with distillate water, dried at room temperature and prepared for FESEM investigation.

The influence of copper introduction and the annealing treatment in the structure of the copper-doped glass ceramics were investigated by X-Ray diffraction (X'Pert Philips diffractometer), using the Bragg Brentano camera geometry with Cu-Kα incident radiation, source voltage and current set at 40 kV and 30 mA, step size Δ(2θ) = 0.02°, fixed counting time of 1 s per step. The obtained spectra were analyzed using the "X'Pert High Score" program, with the PCPDFWIN database (2002 JCPDS- International Centre for Diffraction Data).

The magnetic properties of SC45 and SC45_5Cu were investigated at room temperature in quasi static condition using a DC magnetometer/AC susceptometer (Lakeshore 7225) equipped with a Cryogen-Free Magnet. The measurement of magnetic hysteresis cycle was performed in two different magnetic field ranges: up to 800 kA/m (high field) in order to estimate the main magnetic parameters of the materials and up to 34 kA/m (low field) because such field range could be used in clinical laboratories [17]. The hysteresis cycle area and coercive field were estimated together with the specific power losses (SPL).

The percentage of magnetite crystalized during the glass-ceramic synthesis was determined from the values of saturation magnetization (Ms), using the following formula:

$$\%\, Magnetite = \frac{Ms\ SC45\_5Cu}{Ms\ Magnetite} * 100$$

Where MsSC45_5Cu is the saturation magnetization value of copper doped glass ceramics and Ms Magnetite is saturation magnetization of pure magnetite (purchased by Sigma Aldrich). All Ms values are extrapolated by hysteresis cycle at 800 kA/m.

The glass-ceramics ability to generate heat when exposed to an alternating field was evaluated by means of a magnetic induction furnace (Egma 6 - Felmi S.r.l, Italy), using a working frequency of 220 kHz and a magnetic field of 22.6 mT. The measurements were performed using all samples in powders form for comparison: 0.5 g of glass-ceramic powders were placed in a glass tube containing 16 ml of distilled water, covered with a foam polyethylene thermal insulator to reduce the heat dispersion. The test was performed in triplicate and the temperature increase was measured after 2,4, 6 and 8 min of treatment using a digital thermocouple.

The antibacterial effect of copper-doped samples were investigated using the inhibition halo test, performed in accordance to National Committee for Clinical Laboratory standard (NCCLS [44]) and using a standard strain of *Staphylococcus aureus* (ATCC 29213). For the test, pellets were prepared for both bulk (previously milled and sieved in the same conditions of powders) and powders samples in order to avoid a possible influence of the grain size. The pellets were prepared by weighing 200 mg of glass ceramic powders and pressing them at 4 tons for 10 seconds in an automatic press (Graseby-Specac T-40). The inhibition halo test was performed by preparing a 0.5 McFarland solution (Phoenix Spec BD McFarland), containing approximately $1*10^8$ colony forming units (CFU)/ml, as described in [39,42]. The 0.5 McFarland suspension was uniformly spread on Mueller Hinton agar plate; the samples were placed in contact with the agar and incubated overnight at 35 °C. Subsequently, the inhibition zone was observed and eventually measured.

3. Results and discussion

3.1 Morphological and compositional analysis

The results of FESEM-EDS analysis performed on SC45_5Cu bulk and powders are reported in Figure 1 and 2. The bulk sample showed the presence of micrometric crystals embedded in a glass matric (Figure 1a); the EDS analysis (Figure 1b) evidenced all the peaks characteristic of the glass-ceramics including copper in amount (2.3 at%) slighter lower than the theoretical one. The analysis at higher magnification evidenced the formation of elongated columns of octahedral crystals of magnetite (face centered cubic inverse spinel structure), as already observed in undoped glass-ceramic in previous work [26,28], together with different

crystalline phases having almost cubic or with a cross-like shape and a sort of distorted magnetite crystals (Figure 1c,e). Compositional analyses of the different crystalline phases (Figure 1d,f) showed a higher amount of Fe and the presence of copper, introducing the hypothesis that the copper ions entered into the magnetite unit cell creating modified crystals. Moreover, the analysis in backscattered mode (Figure 1g) demonstrated the presence of nanometric bright particles rich in copper (Figure 1h), often in the center of modified magnetite crystals. This suggests the formation also of copper nanoparticles during the Cu-doped glass-ceramic synthesis. As previously observed by the authors [42] and as reported by Sharma et al. [45] metallic elements can have a nucleating effect on magnetite crystals.

FESEM analysis of SC45_5Cu powders (Figure 2a,e,g) showed always the presence of crystalline phases with different shape and EDS spectrum (Figure 2b) demonstrated the effective introduction of copper (about 2 at%). Also in this case, backscattered images and compositional analysis showed the possible formation of copper nanoparticles (Figure 2c,d). The analysis carried out in the apparently amorphous area evidenced the presence of a Cu and Fe (since a part of iron oxide remains in the glassy matrix and does not crystallize, as reported in [28]), together with the elements characteristic of the glass matrix (Si, Na, Ca and P).

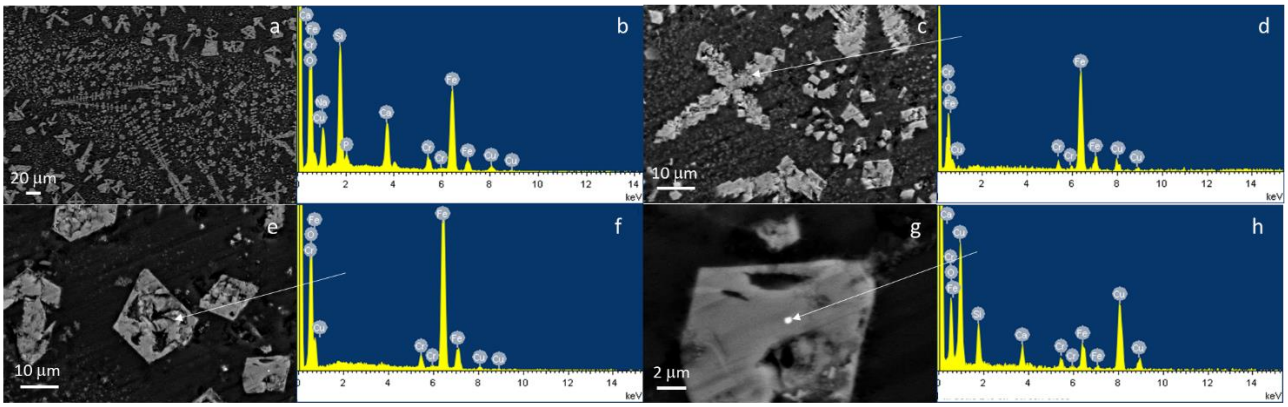

Figure 1: FESEM-EDS analysis of SC45_5Cu bulk .

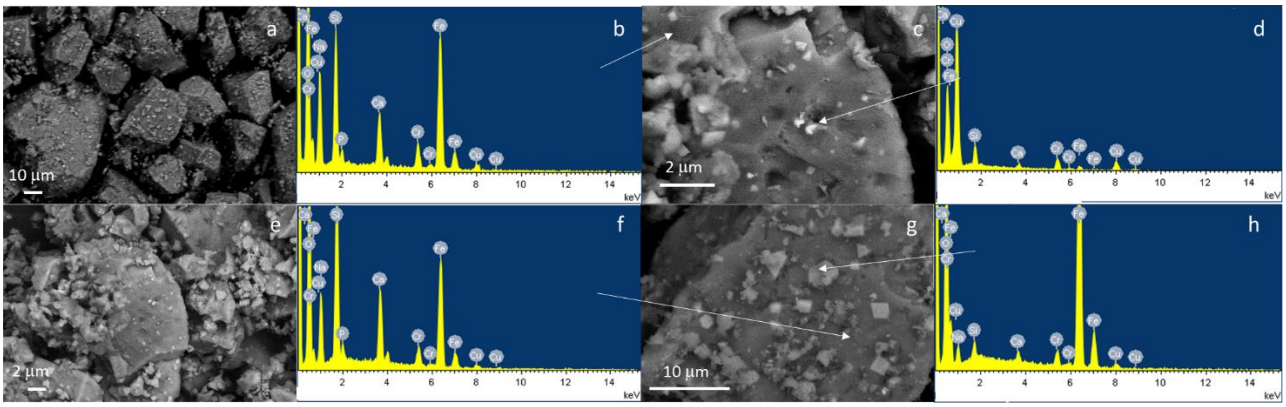

Figure 2: FESEM-EDS analysis of SC45_5Cu powders.

3.2 Phase analysis

The phase analyses of SC45 and SC45_5Cu powders and bulk are shown in Figure 3. The spectra of pristine glass-ceramic SC45 (bulk and powders), as already reported [15], show the presence of magnetite as the main crystalline phase, the amorphous halo between 25 and 35 degrees, related to the residual glassy phase and a small amount of hematite, due to a few decomposition of magnetite during cooling in air. The spectrum concerning SC45_5Cu samples in bulk form evidences also small peaks at about 2 Theta = 31.3° and 40.2° and 55.2°, ascribable to copper iron oxide($CuFeO_2$); as already observed by Abdel-Hameed et al. [46] the copper introduction in a magnetic glass-ceramic containing magnetite can induce the precipitation of delaffosite. While SC45_5Cu powders shows the presence of sodium iron silicon oxide ($FeNaSiO_2$ in non-stoichiometric ratio), evidencing significative differences between the bulk and the powders.

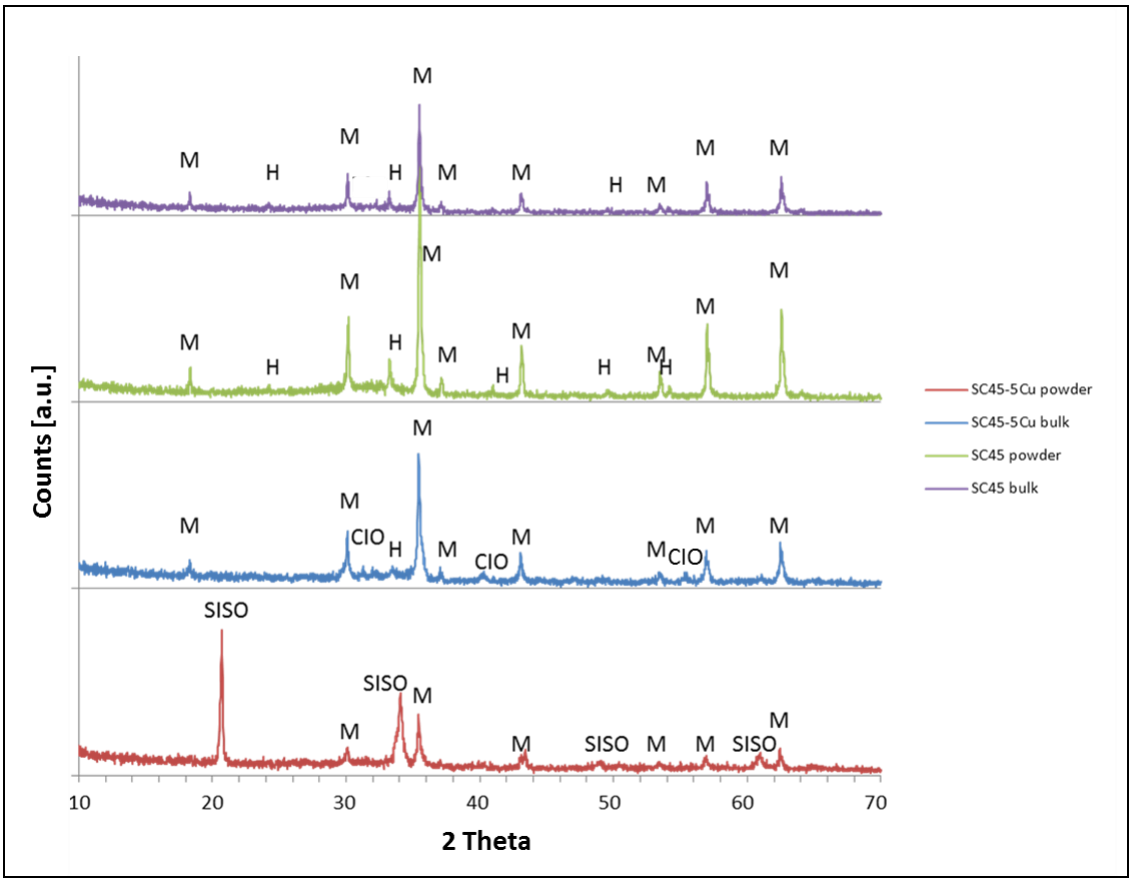

Figure 3: XRD spectra of pristine SC45 (bulk and powders) and SC45_5Cu (bulk and powders). The crystallographic peaks are identified with M magnetite, H hematite , CIO copper iron oxide($CuFeO_2$) , SISO sodium iron silicon oxide ($FeNaSiO_2$ in non-stoichiometric ratio).

3.3 Magnetic and induction heating properties

Figure 4 shows the hysteresis area ratio (as compared with a magnetite sample hysteresis area) and coercive field for hysteresis cycles up to 34 kA/m (low field) for different glass-ceramic samples. It is evident a very low hysteresis area for the powders containing Cu, if compared with the other samples, while some small difference in coercive field was observed.

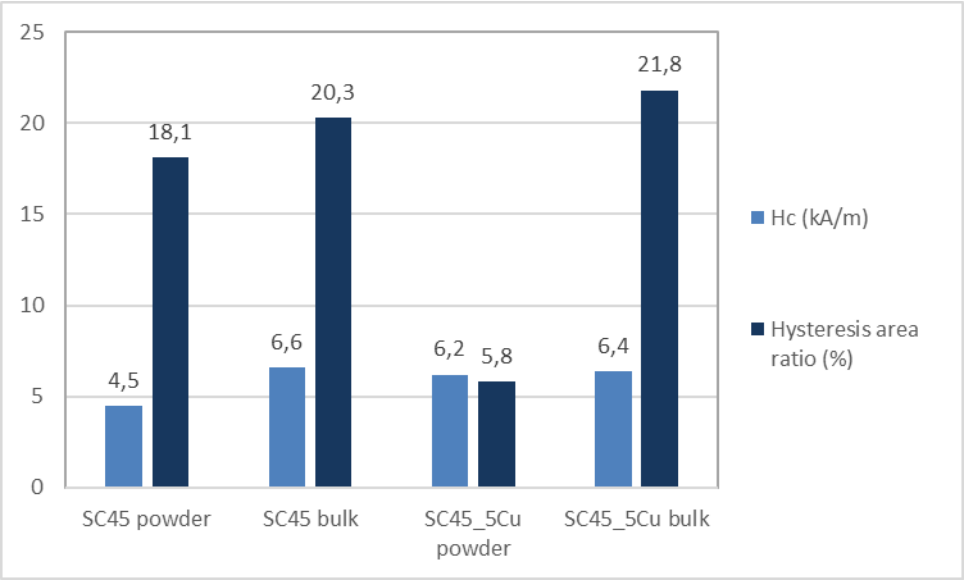

Figure 4. Hysteresis area ratio (as compared with a magnetite sample hysteresis area) and coercive field for hysteresis cycles up to 34 kA/m (low field) for different glass-ceramic samples.

Figure 5 shows the results of calorimetric test performed using an induction furnace. As it can be observed, the ability to release heat of SC45_5Cu in powders form is significantly lower than the pristine glass-ceramic and the SC45_5Cu bulk. This behavior can be due to the presence of low amount of magnetic phase, as evidenced by XRD analysis (Figure 3) and confirmed by the evaluation of magnetite percentage (Figure 6).

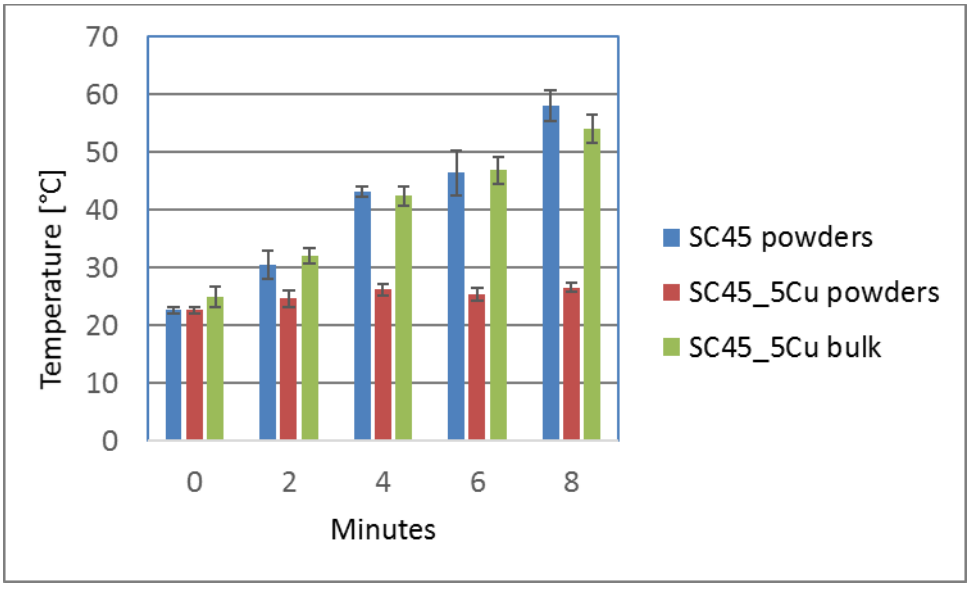

Figure 5. Temperature increment registered during the calorimetric test on SC45 powders, SC45_5Cu powders and bulk.

As it can be observed, the calculation of magnetite percentage using the Ms values, extracted from the hysteresis cycles (Figure 6), demonstrated that copper introduction limited the formation of magnetite, probably fostering the formation of sodium iron silicon oxide (SC45_5Cu powders sample). While the annealing treatment, necessary to prepare SC45_5Cu bulk, allowed a rearrangement of the crystalline phases increasing the magnetite amount, as already observed by other authors [47].

Thus, by combining XRD, calorimetric test and the magnetite amount evaluation it is possible to assess that the magnetic response and released heat of the SC45_5Cu powders are less intense due to the low amount of magnetite nucleated in the sample. On the contrary, the annealed SC45_5Cu bulk samples, containing a higher amount of magnetite, maintained of the magnetic properties and the ability to dissipate heat.

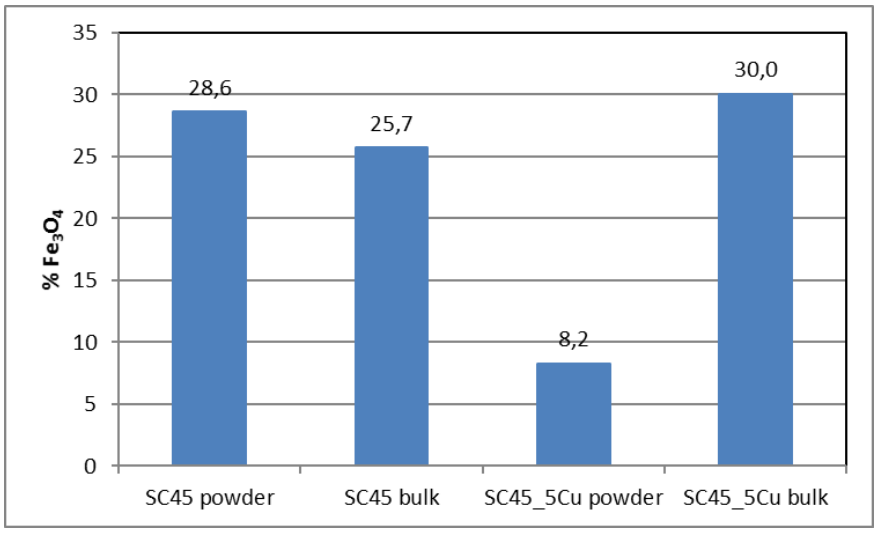

Figure 6: magnetite percentage in different glass-ceramic samples, obtained by the evaluation saturation magnetization values.

3.4 Antibacterial properties

The results of antibacterial test are shown in Figure 7. As it can be noticed, both SC45_5Cu bulk (powered) and powders were unable to limit the bacteria proliferation; in fact, after 24 hours of incubation a blue halo, due to the copper diffusion in the plate, is observable around the samples, more evident for 5Cu bulk sample, but there is no evidence of an inhibition halo formation. This means that copper is released in the agar; however, its amount is not sufficient to avoid bacteria proliferation, even if no bacterial growth was observed by inspecting the back of the plate. As evidenced by the authors in another work [48], the presence of Cu-containing crystalline phases, as well as the formation of Cu nanoparticles evidenced by FESEM analysis, could reduce the antibacterial effect of the materials, confirming that the antibacterial effect is mainly related to the presence of free copper ions in the residual glass phase.

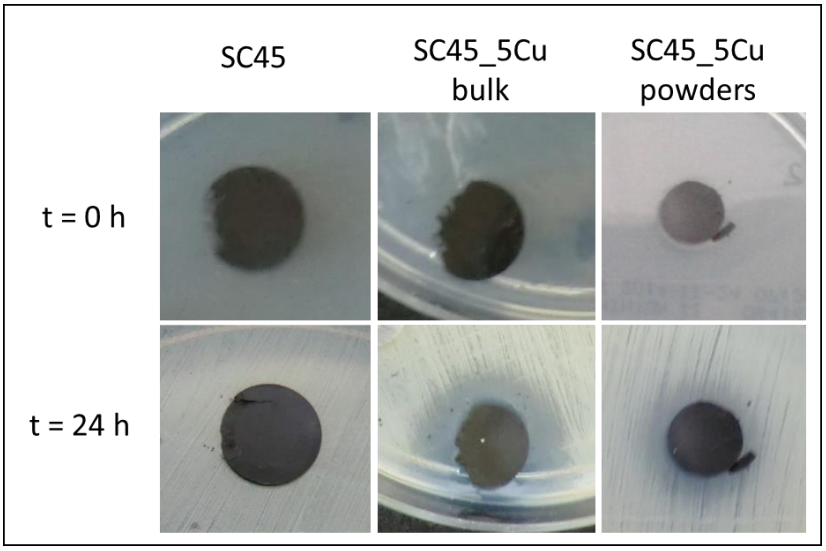

Figure 7: inhibition halo evaluation of pristine glass-ceramic (SC45) and SC45_5Cu samples.

Conclusions

In this research work, copper was inserted in a bioactive and ferrimagnetic glass-ceramic in order to confer antibacterial effect. The Cu-doped glass-ceramic was produced in powders form as well as bulk, introducing

an annealing step. The copper introduction and the synthesis process significantly influence the formation of magnetite and induce the nucleation of different crystalline phases.

In particular, SC45_5Cu powders contain a great amount of non-stoichiometric sodium iron silicon oxide and a reduced amount of magnetite, which significantly influences the magnetic properties of the materials and the ability to release heat, and so its efficacy in the hyperthermia treatment.

The preliminary investigation of antibacterial properties performed against *S. aureus* shows a diffusion of copper ions but not sufficient to avoid bacteria proliferation. Future work will be focused on the design of magnetic-glass ceramic, exploring new approaches to insert copper to improve the antimicrobial properties and verifying the maintenance of bioactive behavior.

Acknowledgements

The authors would like to acknowledge Dr. Fucale Giacomo (Chemical, Clinical and Microbiological Analyses Dept., CTO, Turin, Italy.) for its assistance during antibacterial test.

References

[1] A.K. Freeman, V.P. Sumathi, L. Jeys, Primary malignant tumours of the bone, Surgery 33 (2015) 26–33. doi:10.1016/j.mpsur.2008.12.009

[2] A.K. Freeman, V.P. Sumathi, Jeys L Metastatic tumours of bone, Surgery (Oxford) 33 (2015) 34–39. doi:10.1016/j.mpsur.2014.10.005

[3] D. Campoccia, L. Montanaro, C.R. Arciola The significance of infection related to orthopedic devices and issues of antibiotic resistance, Biomaterials 27 (2006) 2331–39. doi:10.1016/j.biomaterials.2005.11.044

[4] S. Miwa, T. Shirai, N. Yamamoto, K. Hayashi, A. Takeuchi, K. Igarashi, H.Tsuchiya. Current and Emerging Targets in Immunotherapy for Osteosarcoma. J. Oncology 2019 (2019) 7035045. https://doi.org/10.1155/2019/7035045

[5] D. Cross, J.K. Burmester, Gene Therapy for Cancer Treatment: Past, Present and Future. Clin Med Res. 4(3) (2006)218–227. doi: 10.3121/cmr.4.3.218

[6] https://www.esho.info/index.php?id=116, visited April 2021.

[7] B. Hildebrandt, P. Wust, O. Ahlers, A. Dieing, G, Sreenivasa, T. Kerner, R. Felix, H. RiessThe cellular and molecular basis of hyperthermia, Crit Rev Oncol Hematol. 43(1) (2002) 33-56.

[8] M. Idrees, A.Z. Jebakumar. A Review On Potential Benefits Of Hyperthermia In

The Treatment Of Cancer. Acta Biomedica Scientia. 1(3) (2014) 98-104.

[9] B. Emami, C.W Song. Physiological mechanisms in hyperthermia: a review. Int J Radiat Oncol Biol Phys. 10(2) 1984 289-95. doi: 10.1016/0360-3016(84)90015-4.

[10] A.L.B. Seynhaeve, M. Amin, D. Haemmerich, G.C.van Rhoon, T.L.M.ten Hagen. Hyperthermia and smart drug delivery systems for solid tumor therapy. Advanced Drug Delivery Reviews Volumes 163–164, 2020, Pages 125-144. https://doi.org/10.1016/j.addr.2020.02.004

[11] J.L. Roti. Cellular responses to hyperthermia (40–46°C): Cell killing and molecular events. Int. J. Hyperthermia 24 (2008) 3-15.

[12] M. Dunne, M. Regenold, C. Allen. Hyperthermia can alter tumor physiology and improve chemo- and radio-therapy efficacy. Advanced Drug Delivery Reviews 163–164 (2020) 98-124

[13] X. Liu, Y. Zhang, Y. Wang, W. Zhu, G. Li, X. Ma, Y. Zhang, S. Chen, S.Tiwari, K.Shi, S. Zhang, H.M. Fan, Y.X. Zhao, X.J Liang. Comprehensive understanding of magnetic hyperthermia for improving antitumor therapeutic efficacy. Theranostics 10(8) (2020) 3793-3815. doi:10.7150/thno.40805

[14] D. Chang, M. Lim, J A. C.M. Goos5,6, Ruirui Qiao5, Yun Yee Ng4, Friederike M. Mansfeld1,3,5, Michael Jackson2, Thomas P. Davis5,7 and Maria Kavallaris1, Biologically Targeted Magnetic Hyperthermia: Potential and Limitations. Front Pharmacol. 9 (2018) 831. doi: 10.3389/fphar.2018.00831

[15] O. Bretcanu, E. Verné, M. Cöisson, P. Tiberto, P. Allia, Magnetic properties of the ferrimagnetic glass-ceramics for hyperthermia, J Magn Magn Mater 305 (2006) 529-533. https://doi.org/10.1016/j.jmmm.2006.02.264

[16] O. Bretcanu, E. Verné, M. Cöisson, P. Tiberto, P. Allia, Temperature effect on the magnetic properties of the coprecipitation derived ferrimagnetic glass-ceramics, J Magn Magn Mater 300 (2006) 412- 417. https://doi.org/10.1016/j.jmmm.2005.05.030

[17] O. Bretcanu, S. Spriano, E. Vernè , M. Coisson, P. Tiberto, P. Allia The influence of crystallized Fe3O4 on the magnetic properties of coprecipitation-derived ferrimagnetic glass-ceramic, Acta Biomaterialia 1 (2005) 421-429. DOI: 10.1016/j.actbio.2005.04.007

[18] O. Bretcanu, M. Miola, C. L. Bianchi, I. Marangi, R. Carbone, I. Corazzari, M. Cannas, E.Verné. In vitro biocompatibility of a ferrimagnetic glass-ceramic for hyperthermia application. Materials Science and Engineering C 73 (2017) 778–787. DOI: 10.1016/j.msec.2016.12.105

[19] S.A. Shah, M. Hashmi, S. Alam, Effect of aligning magnetic field on the magnetic and calorimetric properties of ferrimagnetic bioactive glass ceramics for the hyperthermia treatment of cancer, Materials Science and Engineering: C, 31 (2011) 1010-1016. https://doi.org/10.1016/j.msec.2011.02.024

[20] M.Miola, Y.Pakzad, S.Banijamali, S. Kargozar, C. Vitale-Brovarone, A.Yazdanpanah, O.Bretcanu, A. Ramedani, E. Vernè, M. Mozafari. Glass-ceramics for cancer treatment: So close, or yet so far? Acta Biomater. 83 (2019) 55-70. doi: 10.1016/j.actbio.2018.11.013.

[21] M.V. Velasco, M.T. Souza, Murilo C. Crovace, A.J. Aparecido de Oliveira, E.D. Zanotto. Bioactive magnetic glass-ceramics for cancer treatment. Biomedical Glasses 5(1) (2019) 148-177. https://doi.org/10.1515/bglass-2019-0013

[22] S.S. Danewalia, K. Singh. Bioactive glasses and glass–ceramics for hyperthermia treatment of cancer: state-of-art, challenges, and future perspectives, Materials Today Bio 10 (2021) 100100. https://doi.org/10.1016/j.mtbio.2021.100100

[23] Y. Zhu, F. Shang, B. Li, Y. Dong, Y. Liu, M.R. Lohe, N. Hanagata,S. Kaskel. Magnetic mesoporous bioactive glass scaffolds: preparation, physicochemistry and biological properties. J. Mater. Chem. B, 1 (2013) 1279-1288. https://doi.org/10.1039/C2TB00262K

[24] C. Wu, W. Fan, Y. Zhu, M. Gelinsky, J. Chang, G. Cuniberti, V. Albrecht, T. Friis, Y. Xiao, Multifunctional magnetic mesoporous bioactive glass scaffolds with a hierarchical pore structure, Acta biomaterialia, 7 (2011) 3563-3572. https://doi.org/10.1016/j.actbio.2011.06.028

[25] F. Baino, E. Fiume, M. Miola, F. Leone, B. Onida,

F. Laviano, R. Gerbaldo, E. Verné, Fe-Doped Sol-Gel Glasses and Glass-Ceramics for Magnetic Hyperthermia. Materials 11 (2018)173; doi:10.3390/ma11010173

[26] N. Shankhwar, A Srinivasa,. Evaluation of sol-gel based magnetic 45S5 bioglass and bioglass-ceramics containing iron oxide. Mater Sci Eng C Mater Biol Appl. 62 (2016)190-196. doi: 10.1016/j.msec.2016.01.054. Epub 2016 Jan 22.

[27] E. Vernè, M. Miola, S. Ferraris, C.L. Bianchi, A. Naldoni, G. Maina, O, Bretcanu. Surface activation of a ferrimagnetic glass-ceramic for antineoplastic drugs Advanced Biomaterials 12 (2010) B309-319. https://doi.org/10.1002/adem.200980082

[28] M. Bruno, M. Miola, O. Bretcanu, C. Vitale-Brovarone, R. Gerbaldo, F. Laviano, E. Verné, Composite bone cements loaded with a bioactive and ferrimagnetic glass-ceramic. Part I: Morphological, mechanical and calorimetric characterization, J Biomater Appl. 29(2) (2014) 254-267. DOI: 10.1177/0885328214521847

[29] E. Verné, M. Bruno, M. Miola, G. Maina, C. Bianco, A. Cochis, L. Rimondini,Composite bone cements loaded with a bioactive and ferrimagnetic glass-ceramic:Leaching, bioactivity and cytocompatibility, Mat. Sc. Eng, C. 53 (2015) 95-103. DOI: 10.1016/j.msec.2015.03.039

[30] M. Miola, F. Laviano, M. Bruno, A. Lombardi, A. Cochis, L. Rimondini, Composite bone cements for hyperthermia: modeling and characterization of magnetic, calorimetric and in vitro heating properties, Ceram. Int., 12 (2016) 049. https://doi.org/10.1016/j.ceramint.2016.12.049

[31] V. Mourino, J.P. Cattalini, A.R. Boccaccini, Metallic ions as therapeutic agents in tissue engineering scaffolds: an overview of their biological applications and strategies for new developments, J. R. Soc. Interface 9 (2012), 401–419. DOI: 10.1098/rsif.2011.0611

[32] A. Hoppe, N.S. Güldal, A.R. Boccaccini, A review of the biological response to ionic dissolution products from bioactive glasses and glass-ceramics. Biomat. 32 (2011) 2757-2774. https://doi.org/10.1016/j.biomaterials.2011.01.004

[33] A. Hoppe, V. Mouriño A.R. Boccaccini, Therapeutic inorganic ions in bioactive glasses to enhance bone formation and beyond. Biomater. Sci., 1 (2013) 254. https://doi.org/10.1039/C2BM00116K

[34] P.Balasubramanian, L.A. Strobel, U. Kneser, A.R. Boccaccini. Zinc-containing bioactive glasses for bone regeneration, dental and orthopedic applications. Biomedical Glasses 1 (2015) 51-69. https://doi.org/10.1515/bglass-2015-0006

[35] M. Bellantone, L.L. Hench. Bioactive Glass, Bioactivity, FT-IR, Silver, Simulated Body Fluid (SBF), X-Ray Diffraction (XRD). Key Engineering Materials 192-195 (2001) 617-620. DOI: https://doi.org/10.4028/www.scientific.net/KEM.192-195.617

[36] M. Miola, C. Vitale Brovarone, G. Maina, F. Rossi, L. Bergandi, D. Ghigo, S. Saracino, M. Maggiora, R.A. Canuto, G. Muzio, E. Vernè, In vitro study of manganese-doped bioactive glasses for bone regeneration. Mater. Sci. Eng. C. 38 (2014) 107–118.

[37] E. Verne, S. Ferraris, M. Miola, G. Fucale, G. Maina, G. Martinasso, R.A. Canuto, S. Di Nunzio, C. Vitale-Brovarone Synthesis and characterisation of bioactive and antibacterial glass-ceramic Part 1— Microstructure, properties and biological behaviour. Adv. Appl. Ceram. 107 (2008)v234–244. doi: 10.1179/174367508X306532.

[38] E. Vernè, M.Miola, C. Vitale-Brovarone, M. Cannas, S. Gatti,G. Fucale,G. Maina,A. Masseè, S. Di Nunzio , Surface silver-doping of biocompatible glass to induce antibacterial properties. Part I: massive glass / - J. Mat. Sci Mat. Med. –20 (2009) 733-740. DOI: 10.1007/s10856-008-3617-9

[39] M.Miola, E. Verné, Bioactive and Antibacterial Glass Powders Doped with Copper by Ion-Exchange in Aqueous Solutions. Materials 9 (2016) 405; doi:10.3390/ma9060405

[40] S. Miwa, T. Shirai, N. Yamamoto, K. Hayashi, A. Takeuchi, K. Tada, et al. Risk factors for postoperative deep infection in bone tumors. PLoS ONE 12(11) (2017) e0187438. https://doi.org/10.1371/journal.pone.0187438

[41] K. Sudhir Kapoor, R. Thiyam, Management of infection following reconstruction in bone tumors. J Clin Orthop Trauma. 6(4) (2015) 244– 251. doi: 10.1016/j.jcot.2015.04.005

[42] M. Miola, R. Gerbaldo, F. Laviano, M. Bruno, E. Vernè, Multifunctional ferrimagnetic glass–ceramic for the treatment of bone tumor and associated complications. J Mater Sci 52 (2017) 9192–9201. https://doi.org/10.1007/s10853-017-1078-6

[43] A.E.MS Hosny, S.A,. Rasmy, D.S. Aboul-Magd, M.T. Kashef, Z.E. El-Bazza. The increasing threat of silver-resistance in clinical isolates from wounds and burns. Infect Drug Resist. 12 (2019) 1985–2001. doi: 10.2147/IDR.S209881

[44] Performance standards for antimicrobial disk susceptibility tests, approved standard M2-A9, 9th ed. NCCLS, Villanova, PA, USA, 2003.

[45] K. Sharma, S.S. Meena, S. Saxena, S.M. Yusuf, A. Srinivasan, G.P. Kothiyal Structural and magnetic properties of glass-ceramics containing silver and iron oxide, Materials Chemistry and Physics 133 (2012) 144– 150. https://doi.org/10.1016/j.matchemphys.2011.12.085

[46] S.A.M. Abdel-Hameed, M.A.Marzouk, A.E.Abdel-Ghany. Magnetic properties of nanoparticles glass–ceramic rich with copper ions. Journal of Non-Crystalline Solids. 357(24) (2011) 3888-3896. https://doi.org/10.1016/j.jnoncrysol.2011.07.026

[47] T.G. Avancini, M. T. Souza, A.P. Novaes de Oliveira, S. Arcaro, A. Kopp Alves. Magnetic properties of magnetite-based nano-glass-ceramics obtained from a Fe-rich scale and borosilicate glass wastes. Ceramics International 45(4) (2019) b4360-4367. https://doi.org/10.1016/j.ceramint.2018.11.111

[48] M. Miola, E. Bertone, E. Vernè. In situ chemical and physical reduction of copper on bioactive glass surface. Applied Surface Science, 495 (2019) article id. 143559. https://doi.org/10.1016/j.apsusc.2019.143559